PRAMANA
— journal of
physics

© Indian Academy of Sciences

Vol. 69, No. 4
October 2007
pp. 575–587

Perturbative effects on ultra-short soliton self-switching

AMARENDRA K SARMA[1,*] and AJIT KUMAR[2]
[1]Department of Physics, Indian Institute of Technology, Guwahati 781 039, India
[2]Department of Physics, Indian Institute of Technology, New Delhi 110 016, India
[*]E-mail: aksarma@iitg.ernet.in

MS received 15 February 2007; revised 19 June 2007; accepted 7 August 2007

Abstract. A numerical study of ultra-short self-soliton switching along with the corresponding analysis of coupler parameters is carried out for a Kerr coupler with intermodal dispersion. The influence of perturbations like third-order dispersion, self-steepening and intrapulse Raman scattering, on switching characteristics is also studied.

Keywords. Soliton switching; nonlinear directional coupler; intermodal dispersion; third-order dispersion; Raman effect; self-steepening.

PACS Nos 42.65.-k; 42.65.Pc

1. Introduction

Fiber couplers, generally known as directional couplers, have become an essential component of optical fiber technology. They have been used for a multitude of fiber-optic devices which require splitting of an optical field into two coherent but physically separated parts.

After the pioneering work of Jensen [1], Maier [2] and Trillo *et al* [3], nonlinear directional couplers (NLDCs) have been studied extensively [4–20,22–24] in the context of all-optical soliton switching. Jensen showed that one can switch a continuous signal from one core to the other by varying the input power of the signal. The idea when applied to pulse switching led to pulse distortion and break-up, resulting in inefficient switching. Since the nonlinear phase modulation is proportional to the instantaneous intensity, different portions of the pulse envelope switch differently, i.e. not simultaneously, leading to pulse distortion and pulse break-up. The pulse break-up during switching is undesirable because it results in inefficient switching and causes cross-talk of the signals. Trillo *et al* showed that pulse break-up could be avoided, if one used soliton pulse as a signal. The physics behind it can be understood from the fact that the nonlinear phase modulation is constant across the entire soliton pulse, owing to which the pulse switches as a whole, i.e., as a single unit and no pulse break-up takes place. Since the work of Trillo *et al* [3], there has been a great deal of activity in studying various aspects of soliton switching in

NLDCs. In this connection the effect of intermodal dispersion on soliton switching dynamics [5–9,13], multistability of switching behavior [22,23], switching between bistable states of a soliton [24], effect of higher order perturbative terms in the nonlinear Schrödinger equation on soliton switching dynamics [14–20] etc. have also been considered and studied. But rarely in these works the practical aspects of an NLDC are considered and studied properly. Keeping this in mind, in the present work we are interested in the realization of a practical nonlinear fiber coupler in the context of an all-optical soliton switching. It is well-known in the context of coupled mode theory that the coupling length of a coupler depends on the coupling coefficient C, which in turn depends on the core radius r and core-to-core separation a [21]. Couplers maintaining a constant, precise separation between the cores cannot be fabricated with very long lengths. Therefore, we need to have a coupler with very small coupling length. In §3 we have presented our calculations regarding the design of such couplers. We observe that the coupling length is extremely sensitive to the choice of coupler parameters such as core-to-core separation, linear coupling coefficient and the pulse width of the signal applied. Our calculation of the coupler length, which takes into account the above-mentioned dependencies, shows that short coupler length requires femtosecond pulse signals [17,18].

The requirement of femtosecond pulses, in turn, necessitates the inclusion of higher-order perturbative terms, like, the third-order dispersion (TOD), Raman term and the self-steepening term. Apart from these, as established by Chiang [5], intermodal dispersion (IMD) must also be accounted for. Intermodal dispersion results in wavelength dependency of the coupling coefficient, i.e. in coupling coefficient dispersion. We know that a twin-core fiber coupler is a bimodal waveguide structure which supports two supermodes, the even mode with a symmetric field distribution and the odd supermode with an anti-symmetric field distribution. It was argued by Chiang [5] that since there is a dispersion mismatch between the two supermodes one should not disregard the IMD effect as it can significantly alter the switching characteristics of a NLDC. Intermodal dispersion was first observed in 1997 [6], by launching short optical pulses (width of about 1 ps) in one of the cores of a dual-core fiber with center-to-center spacing $a = 4r$. Our calculations in §3 show that IMD is strictly dependent on the coupling coefficient and on the pulse width of the signal applied.

In this work, we have presented numerical analysis of an appropriate mathematical model based on the coupled-mode theory [21]. We have considered all the relevant perturbative effects discussed above. In §2 we present a detailed discussion on the mathematical model. The design parameters of the coupler and some typical calculations are presented in §3. The split-step Fourier method is used to solve the set of coupled partial differential equations, which govern the switching dynamics in the coupler as discussed in §2. Numerical results and discussions are presented in §4.

2. The model

We consider a homogeneous and isotropic nonlinear directional coupler with Kerr nonlinearity, made of two identical single-mode fibers with circular cross-sections. The pulse evolution equation inside the coupler is derived in the framework of

the coupled mode formalism [25], using the standard slowly varying envelope approximation. In doing so, along with the expansion of the frequency-dependent propagation constant $\beta(\omega)$ into a Taylor series around the carrier frequency ω_0,

$$\beta(\omega) = \beta_0 + (\omega - \omega_0)\beta_1 + \frac{1}{2}(\omega - \omega_0)^2\beta_2 + \frac{1}{6}(\omega - \omega_0)^3\beta_3 + ..., \tag{1}$$

where

$$\beta_0 = \beta(\omega_0), \quad \beta_n = \left(\frac{\partial^n \beta}{\partial \omega^m}\right)_{\omega=\omega_0}, \quad n = 1, 2, 3, \ldots . \tag{2}$$

For taking into account fiber dispersion, one also has to expand the frequency-dependent coupling coefficient $C(\omega)$ into a Taylor series around ω_0,

$$C(\omega) = C_0 + (\omega - \omega_0)C_1 + \frac{1}{2}(\omega - \omega_0)^2 C_2 + ..., \tag{3}$$

where

$$C_0 \equiv C(\omega_0), \quad C_n = \left(\frac{\mathrm{d}^n C}{\mathrm{d}\omega^n}\right)_{\omega=\omega_0}, \quad n = 1, 2, 3, ..., \tag{4}$$

to incorporate the influence of IMD on pulse evolution [5]. Since the dominant contribution comes from the first-order coupling constant dispersion [5,7], we consider the first and the second terms only in the expansion (3). As a result, taking into account fiber dispersion up to third-order, we obtain the following perturbed system of coupled nonlinear Schrödinger equation (CNLSE) [25,26]

$$\begin{aligned} &i\left(\frac{\partial A_1}{\partial z} + \beta_1\frac{\partial A_1}{\partial T} + C_1\frac{\partial A_2}{\partial T}\right) - \frac{\beta_2}{2}\frac{\partial^2 A_1}{\partial T^2} - i\frac{\beta_3}{6}\frac{\partial^3 A_1}{\partial T^3} \\ &+\gamma|A_1|^2 A_1 + \frac{i}{\omega_0}\frac{\partial}{\partial T}(|A_1|^2 A_1) - T_{\mathrm{R}} A_1\frac{\partial |A_1|^2}{\partial T} + C_0 A_2 = 0, \end{aligned} \tag{5}$$

$$\begin{aligned} &i\left(\frac{\partial A_2}{\partial z} + \beta_1\frac{\partial A_2}{\partial T} + C_1\frac{\partial A_1}{\partial T}\right) - \frac{\beta_2}{2}\frac{\partial^2 A_2}{\partial T^2} - i\frac{\beta_3}{6}\frac{\partial^3 A_2}{\partial T^3} \\ &+\gamma|A_2|^2 A_2 + \frac{i}{\omega_0}\frac{\partial}{\partial T}(|A_2|^2 A_2) - T_{\mathrm{R}} A_2\frac{\partial |A_2|^2}{\partial T} + C_0 A_1 = 0, \end{aligned} \tag{6}$$

where $A_1$and A_2 are the slowly varying pulse envelopes in core 1 and core 2, respectively. Here, $\gamma = n_2\omega_0/cA_{\mathrm{eff}}$ is the nonlinear parameter, where n_2 is the nonlinear Kerr coefficient (which has a typical value of 2.6×10^{-20} m^2/W for standard silica fiber), c is the speed of light in free space and A_{eff} is the effective core area. Here β_1, β_2 and β_3 are the first-, second- and third-order dispersion coefficients, respectively, and $\omega_0 = 2\pi c/\lambda$ is the carrier frequency. The parameter β_1 is related to the group velocity v_{g} of the pulse by $v_{\mathrm{g}} = 1/\beta_1$, while β_2 governs the effect of group velocity dispersion (GVD). β_3 governs the effects of third-order dispersion and becomes important for ultra-short pulses because of their wide bandwidth. The

term proportional to $1/\omega_0$ is responsible for self-steepening. The intrapulse Raman scattering resulting from the delayed Raman response, is given by the term proportional to $T_{\rm R}$. Here, $T_{\rm R}$ is the Raman response time which we have taken to be 3 fs [25]. Note that for a dual core coupler the overlap between the two individual modes is small and hence we have omitted the nonlinear coupling via cross-phase modulation.

Introducing the usual normalization [25]

$$U_1 = \frac{A_1}{\sqrt{P_0}}, \quad U_2 = \frac{A_2}{\sqrt{P_0}}, \quad \xi = \frac{z}{L_{\rm D}}, \quad \tau = \frac{T - \beta_1 z}{T_0}, \tag{7}$$

where $L_{\rm D} = T_0^2/|\beta_2|$, P_0 is the pulse peak power and T_0 is the pulse width of the incident pulse, eqs (1) and (2) can be written in the form

$$i\left(\frac{\partial U_1}{\partial \xi} + \kappa_1 \frac{\partial U_2}{\partial \tau}\right) - \frac{1}{2}\,\mathrm{sgn}\,(\beta_2)\frac{\partial^2 U_1}{\partial \tau^2} - i\delta_3 \frac{\partial^3 U_1}{\partial \tau^3}$$
$$+N^2|U_1|^2 U_1 + is\frac{\partial}{\partial \tau}(|U_1|^2 U_1) - \tau_{\rm R} U_1 \frac{\partial |U_1|^2}{\partial \tau} + \kappa_0 U_2 = 0, \tag{8}$$

$$i\left(\frac{\partial U_2}{\partial \xi} + \kappa_1 \frac{\partial U_1}{\partial \tau}\right) - \frac{1}{2}\,\mathrm{sgn}\,(\beta_2)\frac{\partial^2 U_2}{\partial \tau^2} - i\delta_3 \frac{\partial^3 U_2}{\partial \tau^3}$$
$$+N^2|U_2|^2 U_2 + is\frac{\partial}{\partial \tau}(|U_2|^2 U_2) - \tau_{\rm R} U_2 \frac{\partial |U_2|^2}{\partial \tau} + \kappa_0 U_1 = 0. \tag{9}$$

The parameters N, $\kappa_1, \delta_3, s, \tau_{\rm R}$ and κ_0 are defined as [25]

$$N^2 = \frac{L_{\rm D}}{L_{\rm NL}} = \frac{\gamma P_0 T_0^2}{|\beta_2|}, \quad \text{where } L_{\rm NL} = \frac{1}{\gamma P_0},$$
$$\kappa_1 = \frac{C_1 L_{\rm D}}{T_0}, \quad \delta_3 = \frac{\beta_3}{6|\beta_2|T_0}, \quad s = \frac{1}{\omega_0 T_0}, \quad \tau_{\rm R} = \frac{T_{\rm R}}{T_0}, \quad \kappa_0 = C_0 L_{\rm D}. \tag{10}$$

Thus, $\kappa_0, \kappa_1, \delta_3, s$ and $\tau_{\rm R}$ are respectively the linear coupling constant, the IMD, the TOD, the self-steepening and the Raman coefficients in the normalized unit. The parameter N is called the order of the soliton. N can be eliminated from eqs (8) and (9) by introducing $u_1 = NU_1$ and $u_2 = NU_2$. Thus, the nondimensional system of CNLSE, for the case of anomalous dispersion ($\beta_2 < 0$) is given by

$$i\left(\frac{\partial u_1}{\partial \xi} + \kappa_1 \frac{\partial u_2}{\partial \tau}\right) + \frac{1}{2}\beta_2 \frac{\partial^2 u_1}{\partial \tau^2} - i\delta_3 \frac{\partial^3 u_1}{\partial \tau^3}$$
$$+|u_1|^2 u_1 + is\frac{\partial}{\partial \tau}(|u_1|^2 u_1) - \tau_{\rm R} u_1 \frac{\partial |u_1|^2}{\partial \tau} + \kappa_0 u_2 = 0, \tag{11}$$

$$i\left(\frac{\partial u_2}{\partial \xi} + \kappa_1 \frac{\partial u_1}{\partial \tau}\right) + \frac{1}{2}\beta_2 \frac{\partial^2 u_2}{\partial \tau^2} - i\delta_3 \frac{\partial^3 u_2}{\partial \tau^3}$$
$$+|u_2|^2 u_2 + is\frac{\partial}{\partial \tau}(|u_2|^2 u_2) - \tau_{\rm R} u_2 \frac{\partial |u_2|^2}{\partial \tau} + \kappa_0 u_1 = 0. \tag{12}$$

The above system of CNLSE is the basic system of equations in this work.

3. Design parameters of the coupler

It is well-known that the coupling coefficient, apart from the geometry of the waveguides of the coupler, also depends on the core-to-core separation of the coupler. The coupling coefficient C in units of inverse meters is given by [21]

$$C = \frac{\sqrt{2\Delta}}{r}\frac{U^2}{V^3}\frac{K_0\left(\frac{a}{r}W\right)}{K_1^2(W)}, \tag{13}$$

where r is the core radius, Δ is the refractive index difference between the fiber core and the cladding, and a is the center-to-center separation between the cores of the coupler. K_0 and K_1 are the modified Bessel functions. The core and cladding parameters V, U and W are given by

$$V = \frac{2\pi}{\lambda} r\sqrt{2n_1\Delta}, \quad U = \sqrt{1 + 2\ln V} \quad \text{and} \quad W = \sqrt{V^2 - U^2},$$

where n_1 is the refractive index of the core. In order to obtain C_1 we need to calculate $\mathrm{d}C/\mathrm{d}\omega|_{\omega=\omega_0}$. Introducing the auxiliary function

$$G = \left[2 + 2W\frac{K_0(W)}{K_1(W)} - W\frac{a}{r}\frac{K_1\left(W\frac{a}{r}\right)}{K_0\left(W\frac{a}{r}\right)}\right] \times \left[1 + \frac{U^2}{W^2}\frac{K_0^2(W)}{K_1^2(W)}\right] - \left[1 + \frac{2K_0^2(W)}{K_1^2(W)}\right], \tag{14}$$

we may write

$$C_1 = \frac{\sqrt{2\Delta}}{\omega_0 r}\frac{U^2}{V^3}\frac{K_0(\frac{a}{r}W)}{K_1^2(W)}G. \tag{15}$$

We have assumed the values of κ_0. Now, using (10), (13) and (15), we can calculate the normalized coefficient κ_1. It can clearly be seen that these parameters depend on the core radius, core-to-core separation and the pulse width. Using the following typical fiber parameters $\beta_2 = -20$ ps^2/km, $r = 5$ μm, $n_1 = 1.45, \Delta = 0.004, V = 2.18$ and $\lambda = 1.55$ μm, we have calculated both κ_1 and the coupling length L_{C}, which is defined as

$$L_{\mathrm{C}} = \frac{\pi}{2\kappa_0}\frac{T_0^2}{|\beta_2|}, \tag{16}$$

for different pulse widths T_0 and core-to-core separation a. It is worthwhile to mention that the above definition of coupling length is strictly in the context of a $\pi/2$ linear coupler. It basically represents the length ξ at which the power completely transfers from the input fiber to the other fiber. Some typical values are provided in table 1. We have also provided the values of the normalized coefficient, τ_{R}, δ_3 and s using eq. (10).

It can clearly be seen from table 1 that the coupling length is extremely sensitive to the choice of the coupler parameters. Also, as mentioned in the Introduction, table 1 shows that short coupler length does require ultra-short femtosecond pulses.

Table 1. Values of coupler parameters.

κ_0	T_0 (fs)	a (μm)	L_c (m)	κ_1	τ_R	δ_3	s
0.1	1000	53.75	786.00	−0.0014	0.003	0.0009	0.0008
	50	34.30	1.9571	−0.0162	0.060	0.0180	0.0164
	30	31.00	0.6993	−0.0240	0.100	0.0300	0.0273
	20	28.45	0.3145	−0.0318	0.150	0.0450	0.0410
	10	24.05	0.0785	−0.0508	0.300	0.0900	0.0820
0.5	1000	48.50	157.20	−0.0061	0.003	0.0009	0.0008
	50	29.16	0.3930	−0.0657	0.060	0.0180	0.0164
	30	25.91	0.1414	−0.0937	0.100	0.0300	0.0273
	20	23.35	0.0629	−0.1218	0.150	0.0450	0.0410
	10	19.00	0.0156	−0.1809	0.300	0.0900	0.0820
1.0	1000	46.25	78.74	−0.0115	0.003	0.0009	0.0008
	50	26.95	0.1962	−0.1186	0.060	0.0180	0.0164
	30	23.50	0.0659	−0.1758	0.100	0.0300	0.0273
	20	21.15	0.0312	−0.2131	0.150	0.0450	0.0410
	10	16.85	0.0078	−0.2994	0.300	0.0900	0.0820

4. Numerical results and discussions

As the set of coupled equations (11) and (12) is not analytically solvable, we solve them numerically by the so-called split-step Fourier method. The linear dispersive part is solved by the fast Fourier transform method and the nonlinear part is solved by the fourth-order Runge–Kutta method with auto-control of the step size for a given accuracy of the results. For a detailed discussion on the split-step Fourier method the readers are referred to chap. 2 of [25].

We calculate the transmission coefficient T, representing the fractional output energy in core 1, according to the formula

$$T = \frac{\int_{-\infty}^{\infty} |u_1(\xi,\tau)|^2 \mathrm{d}\tau}{\int_{-\infty}^{\infty} (|u_1(\xi,\tau)|^2 + |u_2(\xi,\tau)|^2) \mathrm{d}\tau}. \tag{17}$$

In this work we have calculated the transmission coefficient T at end of one coupling length of the coupler as defined in §3. Some typical calculations are provided in table 2.

To analyse the switching process we consider the following initial conditions:

$$u_1(0,\tau) = \sqrt{p_0}\,\mathrm{sec}\,h(\tau), \quad u_2(0,\tau) = 0, \tag{18}$$

as suggested in [7].

In this work the results are presented for κ_0 equal to 0.1, 0.5 and 1.0. They correspond to weak coupling, moderate coupling and strong coupling, respectively in our convention. The corresponding coupler parameters are taken from table 1.

To study how IMD may affect the switching characteristics, in figure 1 we have plotted the transmission coefficient as a function of the normalized input peak

Table 2. Values of switching power and coupling length.

κ_0	T_0 (fs)	p_0	T (%)	P_0 (kW)	L_c (cm)
0.1	10	2.0	71	76.00	7.85
	20	1.125	93	10.67	31.45
	30	1.06	95	4.47	69.93
0.5	20	4.25	70	40.00	6.29
	30	3.25	85	13.70	14.14
	50	2.60	88	3.94	39.30
1.0	30	6.0	68	25.00	6.590
	50	5.0	85	7.60	19.62

power, p_0, for a soliton of pulse width 10 fs and $\kappa_0 = 0.1$. The solid curve (a) shows T as a function of p_0 for the case when no perturbative effects (including IMD) are present, while the dotted curve (b) shows the same for the case when only IMD is taken into account. It is clearly seen that IMD essentially modifies the lower part of the transmission curve. We observe that the transmission coefficient T starts at zero for curve (a), while T starts at a nonzero value for curve (b). In fact, this result has already been reported in [7] and agrees well with what we have obtained. But they have not provided any physical explanation of their results. It may be interpreted as follows: In the absence of IMD the phase-matching condition is completely achieved even at low input peak powers, and as a result, all the soliton energy is coupled to the cross state of the coupler after propagation over one coupling length. On the contrary, the presence of IMD destroys the phase-matching condition even at low peak powers and a small fraction of soliton energy remain in the parallel state after one coupling length. As we increase the input peak power p_0 of the soliton, at a certain value of p_0 an equal energy sharing between the parallel and the cross states is observed. The corresponding value p_c of p_0 is called the critical power for switching. If the input peak power of the soliton is increased beyond p_c, more and more of the soliton energy appears in the parallel state, implying $T \to 1$ and, we say that soliton is getting switched (please see [23], ch. 2 of [7]). As seen in figure 1, the critical power for switching is not affected by IMD.

In figures 2–4, we plot the transmission coefficient as a function of the normalized input peak power for solitons of various pulse widths T_0 and for $\kappa_0 = 0.1, 0.5$ and 1.0 respectively. It should be noted that the pulse duration is actually varied via the nondimensionalization (7). Changing T_0 changes the nondimensional reduced time τ, so that pulses of different durations are considered via systems (11) and (12) through a reduced different time scale τ. Here we consider the simultaneous presence of all the perturbative effects. We note from these transmission curves that for a given κ_0, the critical power of switching increases with decrease in the pulse width T_0 of the input soliton. It may be understood from the fact that for a given κ_0 as the pulse width decreases IMD coefficient increases (see table 1) and this results in increase in the coupling coefficient $C(\omega)$. As the critical power of switching is given by $P_c = 4C/\gamma$ in real units [26], it is quite evident that increase in C results in increase in P_c. In addition, it is clear from the transmission curves that the

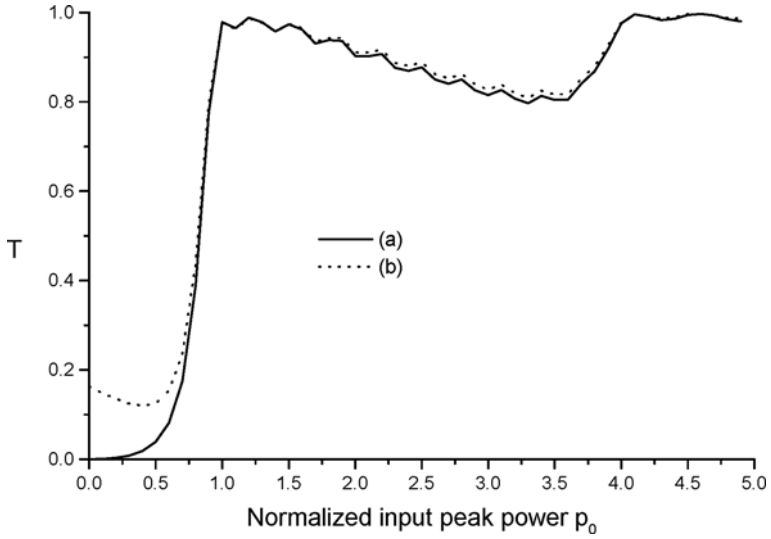

Figure 1. Plot of the transmission coefficient as a function of the normalized input peak power for soliton of pulse width 10 fs with $\kappa_0 = 0.1$. Curve (a) corresponds to the case without any perturbative effects including IMD and curve (b) corresponds to the case when only IMD is taken into account.

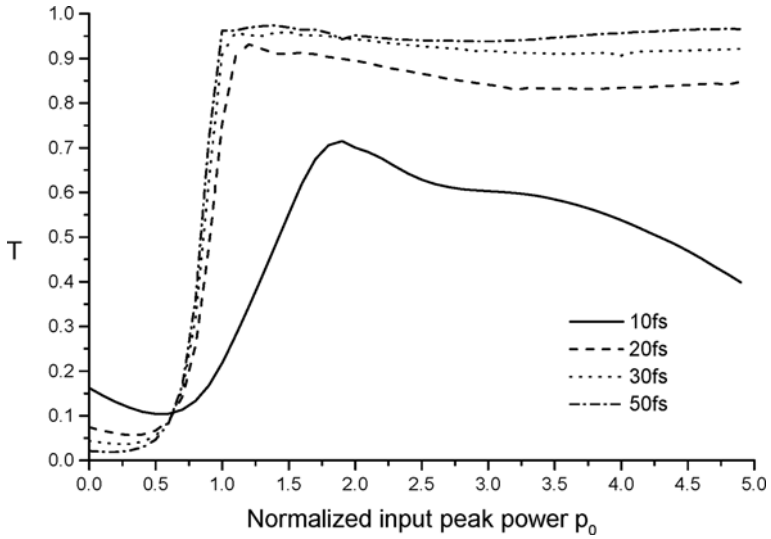

Figure 2. Plot of the transmission coefficient as a function of the normalized input peak power for solitons of various pulse widths T_0. Here the coupling coefficient $\kappa_0 = 0.1$.

effect of the perturbative terms get more pronounced with the decrease in the pulse width. It is quite obvious from eq. (10) in §2 that the corresponding intensities of the perturbative terms like TOD, Raman effect and self-steepening, increase

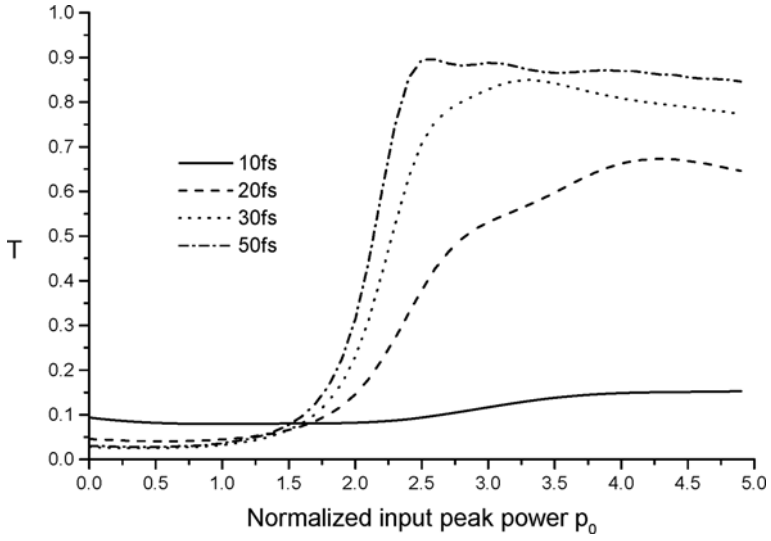

Figure 3. Plot of the transmission coefficient as a function of the normalized input peak power for solitons of various pulse widths T_0. Here the coupling coefficient $\kappa_0 = 0.5$.

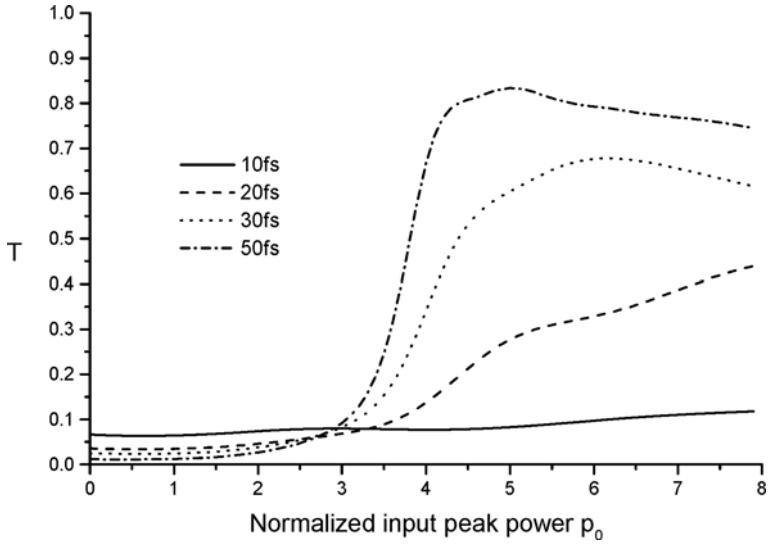

Figure 4. Plot of the transmission coefficient as a function of the normalized input peak power for solitons of various pulse widths T_0. Here the coupling coefficient $\kappa_0 = 1.0$.

with decrease in the input pulse width. Also, we observe that as the coupling coefficient κ_0 increases the influence of the perturbative terms also increases. These perturbative effects adversely affect the switching characteristics of the coupler. These effects become progressively dominant for increasing κ_0 and we observe that

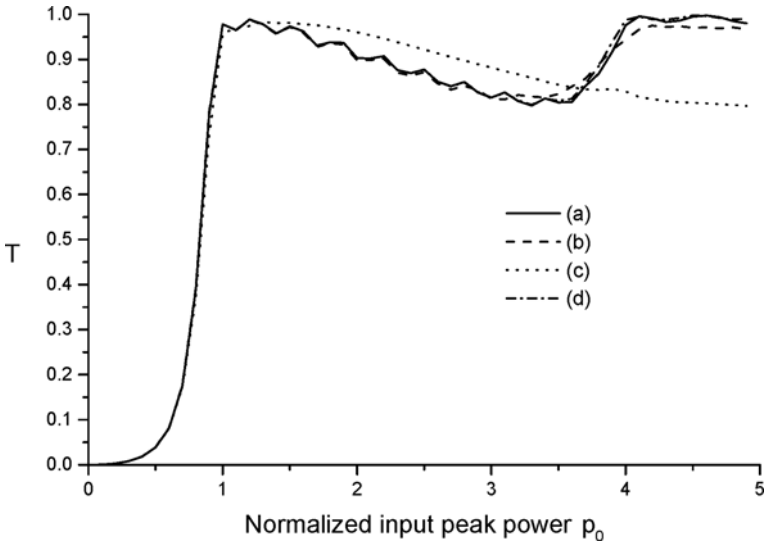

Figure 5. Plot of the transmission coefficient as a function of the normalized input peak power for soliton of pulse width 30 fs with $\kappa_0 = 0.1$. Curve (a) corresponds to the case without any perturbative effects including IMD. Curves (b), (c) and (d) represent respectively the cases when only the TOD, the Raman and the self-steepening effects are taken into account.

for $\kappa_0 = 0.5$ and 1.0 it is not possible to switch a 10 fs soliton pulse. With $\kappa_0 = 1.0$ it is not possible to switch even a 20 fs soliton pulse. It may be expected because with increase in κ_0 the core-to-core separation a decreases and the absolute value of the first-order coupling constant dispersion, κ_1, increases. In other words, IMD does not allow the phase-matching condition to be fulfilled at the input powers considered here. In order to get an idea as to which perturbation plays a major role in the switching performance, we have included the perturbation terms separately and compared their respective transmission coefficients. As an example, in figure 5, we plot the transmission coefficient as a function of the normalized input peak power for $T_0 = 30$ fs and $\kappa_0 = 0.1$. Curve (a) represents the transmission characteristics without any perturbative effects. The curves (b), (c) and (d) correspond to the TOD, the Raman effect and the self-steepening effect only. It can be seen that out of all the perturbative effects, the Raman effect is the most dominant one. As regards the TOD effect is concerned, it is completely negligible in the context of switching. It is because of the very small length scale involved. In fact, we observe that it is mainly due to the Raman effect, that the upper part of the transmission curve is modified [15,16].

Before going further, let us see the order of magnitudes of physical parameters that are required for practical implementation of a soliton switch based on our study. In table 2 we have presented some typical values based on our study of switching characteristics. We see from table 2 that, depending on what we need for a particular application, a trade-off between various parameters of the coupler and the switching characteristics has to be reached. For example, (1) if we take

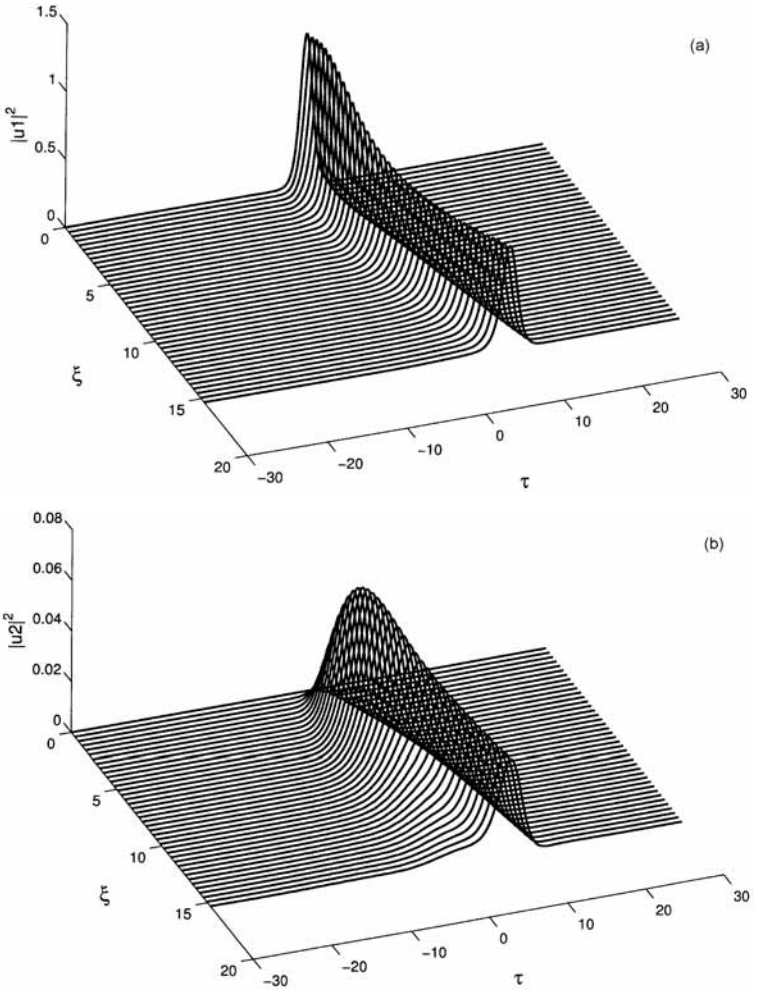

Figure 6. (**a**) Evolution of a 20 fs soliton pulse inside the coupler in core 1 (parallel state of the coupler) with $\kappa_0 = 0.1$. (**b**) Evolution of a small soliton with some radiation leaked into core 2 (crossed state of the coupler) with $\kappa_0 = 0.1$.

$\kappa_0 = 0.1$ and $T_0 = 20$ fs, the required coupler length will be $L_c = 31.45$ cm and for a core radius of 5 μm the core-to-core separation turns out to be $a = 28.45$ μm. For this case we conclude from figure 2 that around 95% switching is possible for $p_0 = 1.125$ which, in real units, corresponds to 10 kW of switching power [20]. On the other hand, (2) if we take $\kappa_0 = 1.0$ and $T_0 = 50$ fs, we can have a lesser switching power ($\approx$7.6 kW) and a smaller coupler length ($\approx$19.62 cm) but then the transmittivity also reduces to about 85%. Therefore the choice, as stated above, depends on a particular requirement, as the case may be.

Finally, in order to have an idea about the behavior and stability of a soliton pulse during propagation inside the coupler, in figure 6, we have depicted the spatio-temporal evolution of the 20 fs soliton pulse of example 1 above. Figure 6a shows soliton evolution in core 1 while figure 6b shows the evolution of a small soliton, with some radiation attached leaking into the second core. It can clearly be seen that the soliton is preserved during evolution inside core 1. However, it gets shifted in the temporal domain along the positive time axis. This is a typical behavior, characteristics of soliton evolution under higher-order perturbations, mainly due to the intrapulse Raman scattering effect [15].

5. Conclusions

We have carried out a detailed numerical study of femtosecond soliton switching in a Kerr coupler by taking into account the intermodal dispersion and perturbative effects like the TOD, self-steepening and intrapulse Raman scattering. To the best of our knowledge we are the first ones to carry out a detailed numerical analysis of the effect of the simultaneous presence of all the perturbative effects on soliton switching in a twin-core fiber coupler. In this connection we have determined the coupler parameters, namely, the coupling length and core-to-core separation as well as the first-order coupling constant dispersion coefficient. Our calculations show that for useful switching characteristics, it is preferable to use shorter pulses and, a compromise between switching power and coupling length can be made depending on our requirement, as shown in table 2. As discussed, with judicious choice of the pulse and coupler parameters one can have transmission up to 95%.

Acknowledgements

The authors would like to thank the referee for his comments which helped in improving the presentation of our work.

References

[1] S M Jensen, *IEEE J. Quantum Electron.* **QE-18**, 1580 (1982)
[2] A A Maier, *Kvant. Electron. (Moscow)* **9**, 2296 (1982)
[3] S Trillo, S Wabnitz, E M Wright and G I Stegeman, *Opt. Lett.* **13**, 672 (1988)
[4] C Paré and M Florjańczyk, *Phys. Rev.* **A41**, 6287 (1990)
[5] K S Chiang, *Opt. Lett.* **20**, 997 (1995)
[6] K S Chiang, Y T Chow, D J Richardson, D Taverner, L Dong, L Reekie and K M Lo, *Opt. Commun.* **143**, 189 (1997)
[7] P M Ramos and C R Paiva, *IEEE J. Quantum Electron.* **QE-35**, 983 (1999)
[8] Ajit Kumar and Amarendra K Sarma, *Opt. Commun.* **234**, 427 (2004)
[9] Y Wang and W Wang, *J. Lightwave Technol.* **24**, 1041 (2006)
[10] Y Fang and J Zhou, Effects of third-order dispersion on soliton switching in fiber nonlinear directional couplers, *Optik* (in press) (2006), http://www.sciencedirect.com
[11] Ajit Kumar and Amarendra K Sarma, *Jpn. J. Appl. Phys.* **44**, 8498 (2005)

[12] Theo P Valkering, Joost van Honschoten and Hugo J W M Hoekstra, *Opt. Commun.* **159**, 215 (1999)
[13] Sotiris Droulias, Manos Manousakis and Kyriakos Hizanidis, *Opt. Commun.* **240**, 209 (2004)
[14] I M Skinner, G D Peng, B A Malomed and P L Chu, *Opt. Commun.* **113**, 493 (1995)
[15] B A Umarov, F Kh Abdullaev and M K B Wahiddin, *Opt. Commun.* **162**, 340 (1999)
[16] G Ingledew, N F Smyth and A L Worthy, *Opt. Commun.* **218**, 255 (2003)
[17] A Mostofi, B A Malomed and P L Chu, *Opt. Commun.* **137**, 244 (1997)
[18] A Mostofi, B A Malomed and P L Chu, *Opt. Commun.* **145**, 274 (1998)
[19] P Shum, K S Chiang and W A Gambling, *IEEE J. Quantum Electron.* **QE-35**, 79 (1999)
[20] Kazuya Shiga, Nishikawa, Kzutoshi Andoh, Masaaki Imai and Yoh Imai, *Mem. Muroran Inst. Tech.* **54**, 101 (2004)
[21] A W Snyder and J D Love, *Optical waveguide theory* (Chapman and Hall, London, 1983) ch. 12–15
[22] A B Aceves and M Santagiustina, *Phys. Rev.* **E56**, 1113 (1997)
[23] K Z Norbrega, M G da Silva and A S B Sombra, *Opt. Commun.* **162**, 340 (2000)
[24] Ajit Kumar and T Kurtz, *J Opt. Soc. Am.* **B18**, 897 (2001)
[25] G P Agrawal, *Nonlinear fiber optics*, second ed. (Academic Press, New York, 2000)
[26] G P Agrawal, *Application of nonlinear fiber optics*, second ed. (Academic Press, New York, 2000)